approximation for carbon and seriously overestimated for uranium. Essentially the same b values are obtained for incident electrons and photons. For many purposes it is sufficient to take $b \approx 0.5$.

The gamma distribution is very flat near the origin, while the EGS4 cascade (or a real cascade) increases more rapidly. As a result Eq. (10.24) fails badly for about the first two radiation lengths; it was necessary to exclude this region in making fits.

Because fluctuations are important, Eq. (10.24) should be used only in applications where average behavior is adequate. Grindhammer *et al.* have developed fast simulation algorithms in which the variance and correlation of a and b are obtained by fitting Eq. (10.24) to individually simulated cascades, then generating profiles for cascades using a and b chosen from the correlated distributions [37].

Measurements of the lateral distribution in electromagnetic cascades are shown in Refs. 32 and 33. On the average, only 10% of the energy lies outside the cylinder with radius R_M. About 99% is contained inside of $3.5R_M$, but at this radius and beyond composition effects become important and the scaling with R_M fails. The distributions are characterized by a narrow core, and broaden as the shower develops. They are often represented as the sum of two Gaussians, and Grindhammer [37] describes them with the function

$$f(r) = \frac{2r\,R^2}{(r^2 + R^2)^2} \ , \tag{10.26}$$

where R is a phenomenological function of x/X_0 and $\ln E$.

10.9. Muon energy loss at high energy

At sufficiently high energies, radiative processes become more important than ionization for all charged particles. For muons and pions in materials such as iron, this "critical energy" occurs at several hundred GeV. Radiative effects dominate the energy loss of energetic muons found in cosmic rays or produced at the newest accelerators. These processes are characterized by small cross sections, hard spectra, large energy fluctuations, and the associated generation of electromagnetic and (in the case of photonuclear interactions) hadronic showers. As a consequence, at these energies the treatment of energy loss as a uniform and continuous process is for many purposes inadequate.

It is convenient to write the average rate of muon energy loss as [38]

$$-dE/dx = a(E) + b(E)\,E \ . \tag{10.27}$$

Here $a(E)$ is the ionization energy loss given by Eq. (10.1), and $b(E)$ is the sum of e^+e^- pair production, bremsstrahlung, and photonuclear contributions. To the approximation that these slowly-varying functions are constant, the mean range x_0 of a muon with initial energy E_0 is given by

$$x_0 \approx (1/b)\ln(a + bE_0) \ . \tag{10.28}$$

Figure 10.10 shows contributions to $b(E)$ for iron. Since $a(E) \approx 0.002$ GeV g^{-1} cm^2, $b(E)E$ dominates the energy loss above several hundred GeV, where $b(E)$ is nearly constant. The rate of energy loss for muons in hydrogen, uranium, and iron is shown in Fig. 10.11 [39].

QED calculations of cross sections for bremsstrahlung and e^+e^- pair production have long been known, but were much improved around 1970 to meet the needs of cosmic ray physics [40–44]. Rozental showed that the screened atomic electron contribution could be included by replacing Z^2 with $Z(Z+1.2)$ in the nuclear bremsstrahlung cross sections and by $Z(Z+1.3)$ in the case of e^+e^- pair production [45], and that other corrections might reduce the cross section by as much as 5%. We take this as the present uncertainty. Cross sections for both processes have been evaluated independently by Tsai [27].

A comparison of various improvements to the Bethe-Heitler formula is given by Wright [46]. For muon energies above 100 GeV, $\mu^+\mu^-$ pair production is also possible. This process is potentially troublesome because it can lead to charge misassignment, but it contributes less than 0.01% to the the total energy loss [39].

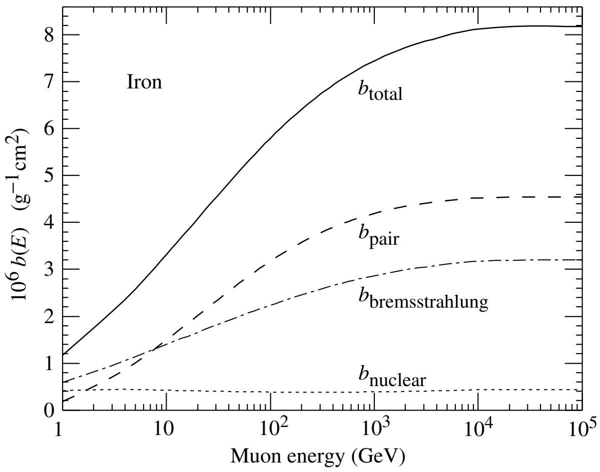

Figure 10.10: Contributions to the fractional energy loss by muons in iron due to e^+e^- pair production, bremsstrahlung, and photonuclear interactions, as obtained from Lohmann *et al.* [39].

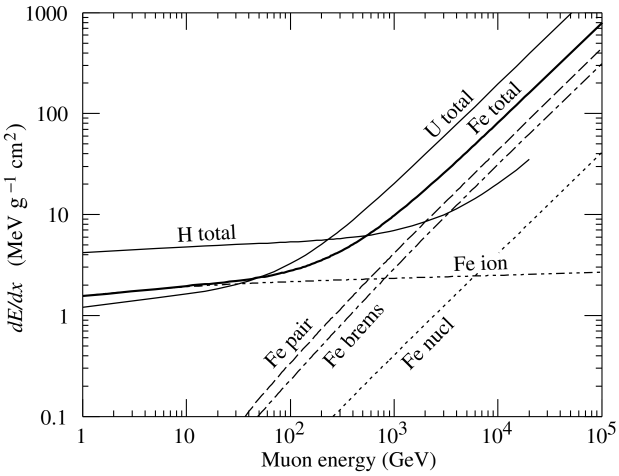

Figure 10.11: The average energy loss of a muon in hydrogen, iron, and uranium as a function of muon energy. Contributions to dE/dx in iron from ionization and the processes shown in Fig. 10.10 are also shown.

Photonuclear interactions account for about 5% of the total energy loss of high-energy muons in iron, and for about 2% in uranium [47]. The losses are concentrated in rare, relatively hard events.

These radiative cross sections are expressed as functions of the fractional energy loss ν. The bremsstrahlung cross section goes roughly as $1/\nu$ over most of the range, while for the pair production case the distribution goes as ν^{-3} to ν^{-2} (see Ref. 48). "Hard" losses are therefore more probable in bremsstrahlung, and in fact energy losses due to pair production may very nearly be treated as continuous. The momentum distribution of an incident 1 TeV/c muon beam after it crosses 3 m of iron is shown in Fig. 10.12. The most probable loss is 9 GeV, or 3.8 MeV g^{-1}cm^2. The full width at half maximum is 7 GeV/c, or 0.7%. The radiative tail is almost entirely due to bremsstrahlung; this includes most of the 10% that lost more than 2.8% of their energy. Most of the 3.3% that lost more than 10% of their incident energy experienced photonuclear interactions. The latter can exceed nominal detector resolution [49], necessitating the reconstruction of lost energy. Electromagnetic and hadronic cascades in detector materials can obscure muon tracks in detector planes and reduce tracking efficiency [50].